A METHOD OF ESTIMATION OF ELASTIC PROPERTIES AND THICKNESSES OF SOIL LAYERS USING VERTICAL HARMONIC LOADING ON GROUND SURFACE AND ITS NUMERICAL VERIFICATION

S. Saitoh[1], T. Harada[2], H. Wang[3], G. Mori[4], and N. Yamashita[5]

[1] *Graduate Student, Systems Engineering, University of Miyazaki, Miyazaki, Japan*
Email: saitoh@civil.miyazaki-u.ac.jp
[2] *Professor, Dept. of Civil and Environmental Engineering, University of Miyazaki, Miyazaki, Japan*
Email: harada@civil.miyazaki-u.ac.jp
[3] *Research Engineer, Earthquake Engineering Research Center Inc., University of Miyazaki, Miyazaki, Japan*
Email: wang@eerc.co.jp
[4] *Chief Engineer, Division of Systems Development, Furuno Electric Co., Ltd., Hyogo, Nishinomiya, Japan*
Email: genji.mori@furuno.co.jp
[5] *Associate Professor, Kobe City College of Technology, Kobe, Japan*
Email: yamasita@kobe-kosen.ac.jp

ABSTRACT :

This paper presents a new method that may achieve a more accurate and lower cost estimation of elastic properties and thicknesses of soil deposits. The kernel of the proposed method, being independent of the usually adopted assumption that only one Rayleigh wave mode is dominant, is to use the near field characteristics of all types of P-SV wave motions on the surface of elastic multi-layered half space generated by the vertical harmonic load applied on its surface. The near field wave motions are accurately simulated by the stiffness matrix method as one of more powerful numerical solutions, and then the following two physical quantities, which can be observable in the field, are used in inversion analysis: (1) the predominant frequency for which the dynamic vertical displacement on the soil surface takes a maximum value, and (2) the frequency variation of the phase velocity at a point on the soil surface near the vertical harmonic load. The phase velocity used in the proposed method is a local quantity varying with the location from the vertical load, because of using all types of waves and their modes. To demonstrate the capability and reliability of the proposed method, the numerical examples are presented by using regular and irregular soil profiles.

KEYWORDS: estimation of layered soil deposit, vertical harmonic load, elastic wave propagation, phase velocity, non destructive testing, Rayleigh wave, SASW

1. INTRODUCTION

Elastic waves generated by dynamic load applied on the soil surface provide the low cost methods to determine the elastic properties and thicknesses of soil deposits. A number of methods, like the spectral analysis of surface waves (SASW), have been used in practice for these purposes.

The SASW (for example, Heisey *et al.*, 1982, Nazarian *et al.*, 1984) is a variation of the Rayleigh wave method (Fry, 1963) developed originally to determine the elastic properties of soil deposits, and their variation with depth, for very low levels of strain. The original Rayleigh wave method uses the harmonic load, while the SASW is based on the spectral analysis of the transient time histories of vertical wave motions observed at the two or more multi-receivers on the soil surface generated by the vertical transient impulse with a duration depending on the range of frequencies of interest also applied on the soil surface. From the phase difference between the receivers which are obtained as a function of frequency and interval distance of these receivers, a plot of the phase velocity versus frequency or wavelength can then be obtained which provides the dispersion curves of the Rayleigh wave. The common key assumption in the SASW and the Rayleigh wave method is that the phase velocity versus frequency obtained from the records is interpreted as a dispersion curve of the

Rayleigh wave corresponding to only one dominant mode. This assumption leads to such some conditions that the records of the receivers at long distant locations from the source at least about dx (dx =interval distance of receivers) should be used and also a filtering criterion ($L_R / 3 < dx < 2L_R : L_R$ = Rayleigh wavelength) should be applied for dx of receivers to obtain the dispersion curve (Heisey *et al.*, 1982). These conditions restrict the accuracy of dispersion curve especially in the low frequency range and hence they lead to the inaccurate estimation of deeper soil layers.

This paper presents an alternative method which is independent of the usually adopted assumption that only one Rayleigh wave mode is dominant. This method uses the near field characteristics of all types of P-SV wave motions on the surface of elastic multi-layered half space generated by the vertical harmonic load applied on its surface. The near field wave motions are accurately simulated by the stiffness matrix method (Kausel *et al.*, 1981, Harada *et al.*, 1995, 2005) as one of more powerful numerical solutions, and then the following two physical quantities, which can be observable in the field, are used in inversion analysis: (1) the predominant frequency for which the dynamic vertical displacement on the soil surface takes a maximum value, and (2) the frequency variation of the phase velocity at a point on the soil surface near the vertical harmonic load. It is noted here that the proposed method does not use the filtering criterion such as that suggested by, for example, Heisey *et al.*, (1982), but uses the frequency varying phase velocity closer to the point of harmonic load that can be directly observed from the phase difference of the receivers, because the near field effects and all wave modes are taken into consideration in the proposed simulation. The observed frequency varying phase velocity is interpreted in this paper as a local quantity varying with the location from the vertical load. It should be acknowledged that the advanced development of the computer simulation methods of the full wave motions makes it possible to develop a Rayleigh wave free method of estimation of soil properties and their variation with depth.

2. BRIEF DESCRIPTION OF NUMERICAL ANALYSIS OF WAVE FIELD BASED ON STIFFNESS MATRIX METHOD

Stiffness matrix method was originally developed by Kausel *et al.*, (1981) and are extended to the simulation of seismic wave motions due to the kinematical fault rupture model in the multi-layered half space by Harada *et al.*, (1999, 2005). In this chapter, a brief description of the stiffness matrix method in a Cartesian coordinate system, which is used in the simulation of full wave motions and the estimation of the soil properties and their variation with depth, is presented here (Harada *et al.*, 1999, 2005).

In a Cartesian coordinate system (x, y, z), the displacement vector $\mathbf{u}(x, y, z, t) = (u, v, w)^T$ at time t is retrieved by the three hold Fourier transform as follows,

$$\mathbf{u}(x, y, z, t) = \frac{1}{(2\pi)^3} \int_{-\infty}^{\infty} \int_{-\infty}^{\infty} \int_{-\infty}^{\infty} \mathbf{u}(\kappa_x, \kappa_y, z, \omega) \, \mathrm{e}^{i(\kappa_x x + \kappa_y y - \omega t)} \, d\kappa_x \, d\kappa_y \, d\omega \tag{2.1}$$

where $\mathbf{u}(\kappa_x, \kappa_y, z, \omega)$ is the wave motion displacement vector at depth z in frequency ω and wave number (κ_x, κ_y) domain. The displacement vector $\mathbf{u}(\kappa_x, \kappa_y, z, \omega)$ can be obtained from the SH wave displacement $v_0(\kappa, z, \omega)$ and the P-SV wave displacements $u_0(\kappa, z, \omega), w_0(\kappa, z, \omega)$ such as,

$$\begin{aligned} u(\kappa_x, \kappa_y, z, \omega) &= \frac{\kappa_x}{\kappa} u_0(\kappa, z, \omega) - \frac{\kappa_y}{\kappa} v_0(\kappa, z, \omega) \\ v(\kappa_x, \kappa_y, z, \omega) &= \frac{\kappa_y}{\kappa} u_0(\kappa, z, \omega) + \frac{\kappa_x}{\kappa} v_0(\kappa, z, \omega) \\ w(\kappa_x, \kappa_y, z, \omega) &= w_0(\kappa, z, \omega) \end{aligned} \tag{2.2}$$

where $\kappa = \sqrt{{\kappa_x}^2 + {\kappa_y}^2}$ stands for the wave number in the direction of wave (SH and P-SV waves) propagation. The SH wave displacement $v_0(\kappa, z, \omega)$ and the P-SV wave displacements $u_0(\kappa, z, \omega), w_0(\kappa, z, \omega)$ are obtained by solving the following stiffness matrix equation (linear simultaneous equation), for example, for a three layered half space with an earthquake fault rupture in the 2nd layer,

$$\begin{pmatrix} \boldsymbol{K}_{11}^{(1)} & \boldsymbol{K}_{12}^{(1)} & \mathbf{0} & \mathbf{0} \\ \boldsymbol{K}_{21}^{(1)} & \boldsymbol{K}_{22}^{(1)} + \boldsymbol{K}_{11}^{(2)} & \boldsymbol{K}_{12}^{(2)} & \mathbf{0} \\ \mathbf{0} & \boldsymbol{K}_{21}^{(2)} & \boldsymbol{K}_{22}^{(2)} + \boldsymbol{K}_{11}^{(3)} & \boldsymbol{K}_{12}^{(3)} \\ \mathbf{0} & \mathbf{0} & \boldsymbol{K}_{21}^{(3)} & \boldsymbol{K}_{22}^{(3)} + \boldsymbol{K}_{Half} \end{pmatrix} \begin{pmatrix} \boldsymbol{u_0}(z_0) \\ \boldsymbol{u_0}(z_1) \\ \boldsymbol{u_0}(z_2) \\ \boldsymbol{u_0}(z_3) \end{pmatrix} = \begin{pmatrix} \boldsymbol{q_0}(z_0) \\ \boldsymbol{q_0}(z_1) + \boldsymbol{q_s}(z_1) \\ \boldsymbol{q_0}(z_2) + \boldsymbol{q_s}(z_2) \\ \boldsymbol{q_0}(z_3) \end{pmatrix} \tag{2.3}$$

in which $\mathbf{u}_0(z) \equiv \mathbf{u}_0(\kappa, z, \omega)$ for simplicity of notions, and $\mathbf{K}_{ij}^{(n)}, \mathbf{K}_{Half}$ represent the stiffness matrix of the n-th layer and the half space, respectively. And also $\mathbf{q}_0(z_n), \mathbf{q}_s(z_n)$ stand for the external forces and the earthquake fault rupture based forces in unit area on depth z_n in frequency wave number domain.

3. CHARACTERISTICS OF P-SV FULL WAVE FIELD ON SOIL SURFACE DUE TO VERTICAL HARMONIC LOAD ON SOIL SURFACE

3.1. Definition of Vertical Amplitude and Phase Velocity on Soil Surface

The Eqns. 2.1 to 2.3 can be used to simulate the 3-dimensional wave motions for the case not only of external excitation but also earthquake fault rupture excitation (Harada *et al.*, 1999, 2005). For simplicity in this paper, the 2 dimensional P-SV wave motions due to a vertical harmonic load with amplitude q_0 on the center of the soil surface are simulated and their characteristics are described in terms of the vertical displacement amplitude $|w(x,\omega)|$ and the phase velocity $c(x,\omega)$ on the soil surface ($z_0 = 0$) as a function of the excitation frequency and the distance from the load.

In this case (the simulation of the 2 dimensional P-SV wave motions), the right hand external forces in Eqn. 2.3 are given by,

$$\begin{aligned} \boldsymbol{q_0}(z_0) &= (0, iq_0\delta(\omega - \omega_0)) \\ \boldsymbol{q_0}(z_1) = \boldsymbol{q_0}(z_2) = \boldsymbol{q_0}(z_3) &= \boldsymbol{q_s}(z_1) = \boldsymbol{q_s}(z_2) = \mathbf{0} \end{aligned} \tag{3.1}$$

where δ is a delta function, and ω_0 is the excitation frequency of the vertical harmonic load.

The vertical displacement on soil surface is obtained from the P-SV wave stiffness matrix equation (Eqn. 2.3) and its Fourier transform with respect to the wave number κ as,

$$w(x,t) = q_0 \mathrm{e}^{-i\omega t} \frac{1}{2\pi} \int_{-\infty}^{\infty} w(\kappa, \omega) \mathrm{e}^{i\kappa x} d\kappa = q_0 \mathrm{e}^{-i\omega t} w(x, \omega) \tag{3.2}$$

where $w(x,t) \equiv w_0(x', t), x \equiv x'$ (x'=the axis of P-SV wave propagation) for simplicity of notations. The vertical displacement $w(x,\omega)$ in $x-\omega$ domain in Eqn. 3.2 can be expressed as

$$w(x,\omega) = R[w(x,\omega)] + iI[w(x,\omega)] = |w(x,\omega)| \mathrm{e}^{i\theta(x,\omega)} \tag{3.3}$$

where,

$$|w(x,\omega)| = \sqrt{R^2[w(x,\omega)] + I^2[w(x,\omega)]}$$
$$\theta(x,\omega) = \tan^{-1}\left(\frac{I[w(x,\omega)]}{R[w(x,\omega)]}\right) \tag{3.4}$$

Then substituting Eqn. 3.3 into Eqn. 3.2, $w(x,t)$ can be expressed as

$$w(x,t) = q_0 |w(x,\omega)| e^{-i\omega\left[t - \frac{\theta(x,\omega)}{\omega}\right]} \tag{3.5}$$

The phase velocity, $c(x,\omega) = dx/dt$, can be obtained by differentiating the phase, $\omega t - \theta(x,\omega) = \text{constant}$ with respect to time t in Eqn. 3.5 such as,

$$c(x,\omega) = \frac{\omega}{\dfrac{d\theta(x,\omega)}{dx}} = \frac{2dx \cdot \omega}{\theta(x+dx,\omega) - \theta(x-dx,\omega)} \tag{3.6}$$

3.2. Numerical Example of Characteristics of Vertical Amplitude and Phase Velocity on Soil Surface

For the numerical example of the characteristics of vertical amplitude and phase velocity on soil surface, a single soil layer on half space as shown in Figure 1 is used. In Figure 1, H =thickness of soil layer, ρ =soil mass, V_p, V_s =P wave and S wave velocities, respectively, and Q =Q value representing material damping of soil.

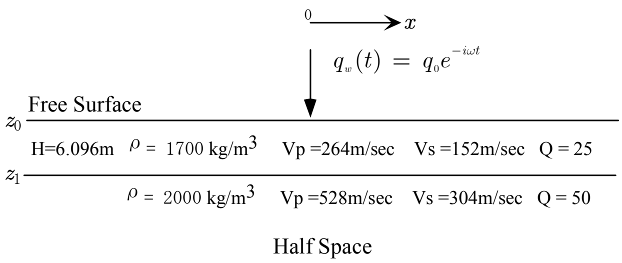

Figure 1 A single soil layered half space subjected to a harmonic load with amplitude q_0 on its surface used in numerical example

Figure 2 shows the vertical displacement amplitude $|w(x,\omega)|$ as a function of distance x ($0 < x < 100\ m$) from the vertical load and the frequency $f = \omega/2\pi$ ($0 < f < 100\ Hz$). In this figure the value of $|w(x,\omega)|/(q_0/\mu)$, where μ=shear modulus of single soil layer, is plotted in terms of a bird's-eye-view (a) and a contour curve map (b) of $|w(x,\omega)|/(q_0/\mu)$.

From Figure 2 a predominant peak of the vertical displacement amplitude is observed at a frequency around 10 Hz, but its amplitude and frequency vary with the distance x from the point of vertical harmonic load. To see the amplitude and frequency variation of $|w(x,\omega)|/(q_0/\mu)$ in detail, Figure 3 indicates $|w(x,\omega)|/(q_0/\mu)$ at the 3 points of distance $x = 5m, 10m, 20m$. The frequency for which the predominant peak appears in $|w(x,\omega)|/(q_0/\mu)$ may be interpreted as the predominant frequency of the soil deposit, but the predominant frequency is slightly varying with the distance x from the load. In this sense the predominant frequency observed in the near field closer to the load is interpreted as a local quantity.

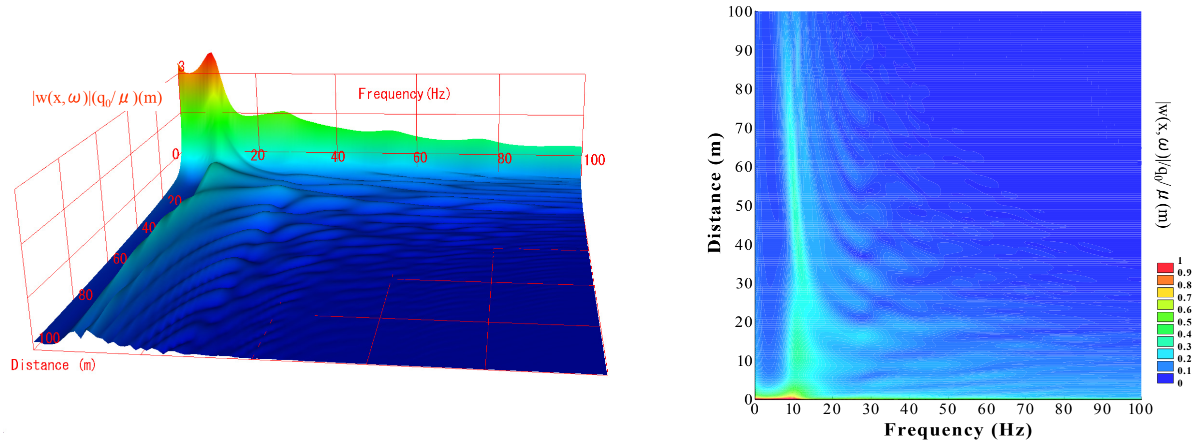

(a) (b)

Figure 2 Normalized vertical displacement amplitude $|w(x,\omega)|/(q_0/\mu)(m)$ in terms of a bird's-eye-view (a) and a contour curve map (b)

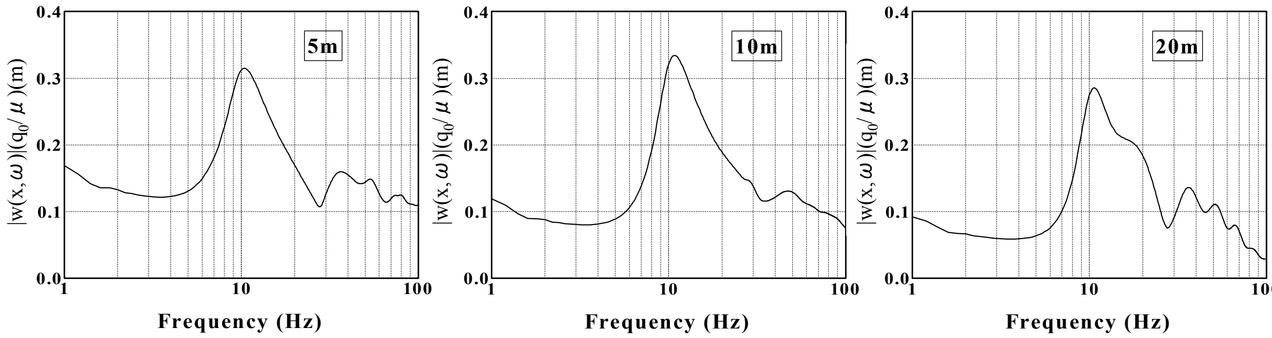

(a) (b) (c)

Figure 3 Normalized vertical displacement amplitudes $|w(x,\omega)|/(q_0/\mu)(m)$ at $x = 5m, 10m, 20m$

Figure 4 shows the phase velocity of $c(x,\omega)$ on the soil surface similarly in terms of a bird's-eye-view (a) and a contour curve map (b) in the range of ($0 < x < 50\ m$, $0 < f < 50\ Hz$). From this figure, the phase velocity exhibits the wavy forms in $x - f$ domain. The variation of the wavy forms is depending on the distance as well as the frequency. The frequency variation of the phase velocity is known as the dispersion curves of Rayleigh wave but in which they are a function of only the frequency and being independent of the distance. It is noted here that the phase velocity versus frequency of the Rayleigh wave at a point far away from the load exhibits also a wavy variation with only the frequency due to the superposition of all modes of Rayleigh wave. Being similar to the vertical displacement amplitude $|w(x,\omega)|/(q_0/\mu)$, also the phase velocity $c(x,\omega)$ is called as the local quantity which varies with both the distance and the frequency. To see more clearly the frequency and distance variation of $c(x,\omega)$ and its relation to the dispersion curves of Rayleigh wave, the phase velocity at the 3 points of distance $x = 5m, 10m, 20m$ and the dispersion curves of the 1st, 2nd, and 3rd modes of the Rayleigh wave are plotted in Figure 5. It is found from Figure 5 that $c(x,\omega)$ never coincides with the dispersion curves of Rayleigh wave, especially in the case of the closer distance of the case (a) $x = 5\ m$, and also in the lower frequency range below the approximate predominant frequency even in the cases (b) and (c). It is noted here that a usually used filtering criterion such as that suggested by Heisey *et al.*, (1982) can be interpreted as a filter device to obtain an approximation of the dispersion curve varying with only the frequency for the predominant mode (usually 1st mode) of Rayleigh wave from the observed phase velocity that is a local quantity exhibiting a variation with the frequency as well as the distance. It should be noted here also that the predominant mode of Rayleigh wave is depending on the soil profiles where the 1st mode may be dominated for the regular soil deposits while the higher modes may become significant for the irregular soil deposits. Therefore the usually used filtering criterion restricts the accuracy of dispersion curve of a irregular soil deposit and also especially in the low frequency range and hence it leads to the inaccurate estimation of deeper soil layers.

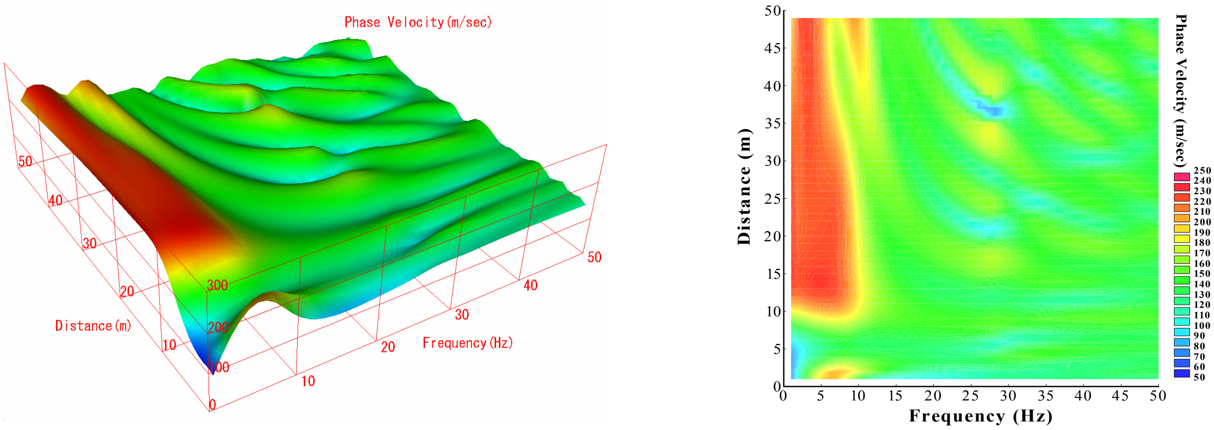

(a) (b)

Figure 4 Phase velocity in terms of $c(x,\omega)$ a bird's-eye-view (a) and a contour curve map (b)

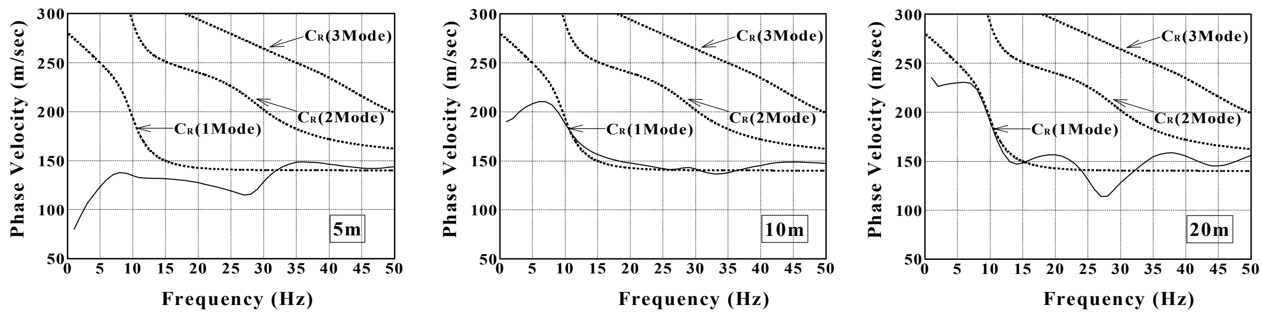

(a) (b) (c)

Figure 5 Phase velocity in terms of $c(x,\omega)$ $x = 5m, 10m, 20m$ and the dispersion curves of Rayleigh wave

4. NUMERICAL EXAMPLE OF ESTIMATION OF SOIL PROPERTIES AND THICKNESSES USING THE NEAR FIELD PAHSE VELOCITY

Figure 6 shows three typical soil layered half space used in this numerical example for the inversion analysis to estimate elastic soil properties and thicknesses of soil deposits, in order to demonstrate that the accurate estimate can be achieved by using the phase velocity observed in the closer points to the harmonic load in conjunction with the simulation method (the stiffness matrix method is used in this paper described in chapter 2 briefly) of all types of P-SV wave motions. As being seen from Figure 6, the three cases are chosen in such a way that they cover both regular (case 1 in Figure 6 (a)) and irregular (cases 2 and 3 in Figure 6 (b) and (c)) soil layered half space. Table 1 shows the thicknesses and elastic properties of the three soil deposits in Figure 6. In this numerical example of inversion analysis, the modified Marquardt method (Marquardt, 1963) is used as a nonlinear minimization technique of the error function as,

$$\varepsilon = \frac{1}{m-n+1}\sum_{i=n}^{m}\left[(y_i - g_i)/C_{S1}^*\right]^2 \tag{4.1}$$

where ε=square error of the phase velocity varying with frequency, n, m=discrete frequency number, y=the phase velocity of the true soil profile, g= the phase velocity of the estimated soil profile, and C_{S1}^*=the S wave velocity of the 1st layer (appropriate value is assumed). In this inversion, the phase velocity at the distance $x = 2\ m$ from the load calculated using Eqn. 3.6 by the phase difference between two receivers of interval $dx = 1\ m$ is used.

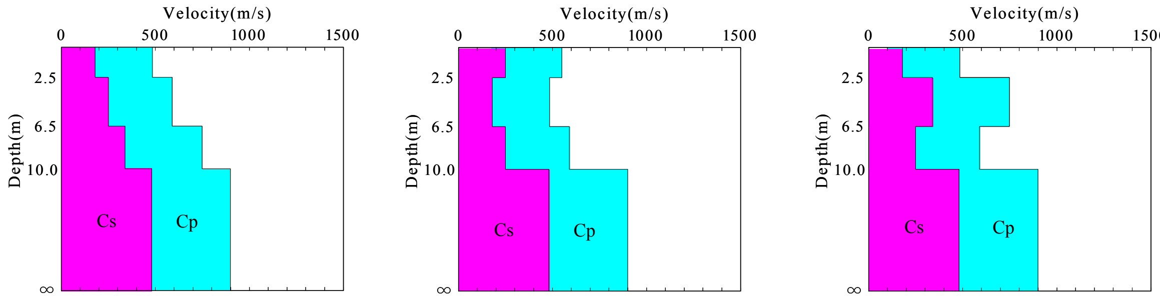

(a) Case1 (b) Case2 (c) Case3

Figure 6 Three typical soil layered half space used in numerical examples (case 1 (a) is regular soil deposits and cases 2 and 3 (b), (c) are irregular soil deposits)

Table 1 Thicknesses and elastic properties of the three soil layered half space of Figure 6

(a) Case1

H(m)	Cp(m/s)	Cs(m/s)	ν	$\rho\,(kg/m^3)$	Q
2.5	484.7	180.0	0.42	1800.0	25
4.0	588.7	250.0	0.39	1800.0	25
3.5	748.5	340.0	0.37	1800.0	25
∞	898.0	480.0	0.30	2000.0	50

(b) Case2

H(m)	Cp(m/s)	Cs(m/s)	ν	$\rho\,(kg/m^3)$	Q
2.5	550.3	250.0	0.37	1800.0	25
4.0	484.7	180.0	0.42	1800.0	25
3.5	588.7	250.0	0.39	1800.0	25
∞	898.0	480.0	0.30	2000.0	50

(c) Case3

H(m)	Cp(m/s)	Cs(m/s)	ν	$\rho\,(kg/m^3)$	Q
2.5	484.7	180.0	0.42	1800.0	25
4.0	748.5	340.0	0.37	1800.0	25
3.5	588.7	250.0	0.39	1800.0	25
∞	898.0	480.0	0.30	2000.0	50

Figure 7 shows the starting soil layered half spaces (initial soil deposits) for the case1 (a) to case3 (c) used in the inversion analysis. These initial soil deposits are appropriately chosen for which the predominant frequency is close to that of the true soil deposits (this predominant frequency is observable). The initial soil deposits are assumed to be a five layered half space, while the true soil deposits is a three layered half space, by considering the number of soil layers is one of the unknown parameters in the initial soil deposits. The unknown parameters, that the inversion analysis in the numerical examples must estimate, are the number of soil layers, the thickness of each soil layer, and the S wave and P wave velocities (or Poisson ratios) in each layer. The soil mass in each soil layer is treated as a known parameter.

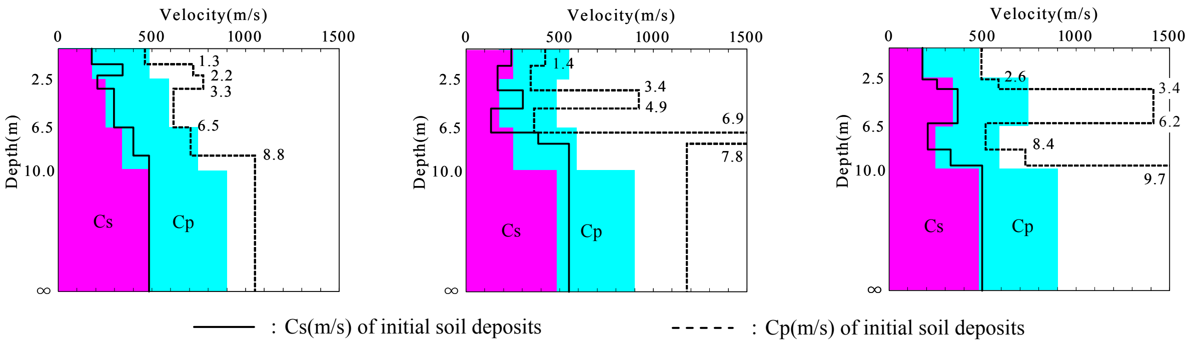

(a) Case1 (b) Case2 (c) Case3

Figure 7 Starting soil layered half spaces (initial soil deposits) for the (a)case1 to the (c)case3

Figure 8 shows the frequency variations of the phase velocity at $x = 2\ m$ for the initial soil deposits and the true soil deposits of case 1 to case 3. By using the nonlinear minimization technique of the square error defined by Eqn. 4.1, the unknown elastic properties and thicknesses of soil deposits described above are estimated so that the difference of the phase velocities of the true and initial soil deposits is minimized. In these numerical examples, we can confirm that the perfect true soil deposits of Figure 6 can be estimated from the initial soil deposits of Figure 7.

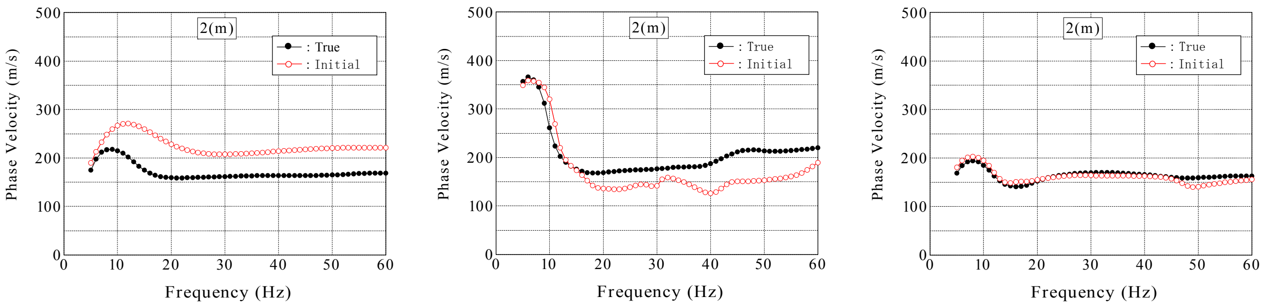

(a) Case1 (b)Case2 (c)Case3

Figure 8 Frequency variations of the phase velocity at $x = 2\ m$ for the initial soil deposits and the true soil deposits of (a)case1 to (c)case3

5. CONCLUSIONS

A new method to estimate elastic properties and thicknesses of soil deposits is presented which is independent of the usually adopted assumption that only one Rayleigh wave mode is dominant. This method uses the near field characteristics of all types of P-SV wave motions on the surface of elastic multi-layered half space generated by the vertical harmonic load applied on its surface. The proposed method does not use the filtering criterion, but uses the frequency varying phase velocity closer to the point of harmonic load that can be directly observed from the phase difference of the receivers, because the near field effects and all wave modes are taken into consideration in the proposed simulation. The observed frequency varying phase velocity is interpreted in this paper as a local quantity varying with the location from the vertical load. To demonstrate the capability and reliability of the proposed method, the numerical examples are presented by using regular and irregular soil profiles.

REFERENCES

Fry, Z. B. (1963). A procedure for determining elastic moduli of soils by field vibratory technique. *U.S. Army Engineer Waterway Experiment Station*, Miscellaneous Paper 4.

Harada, T., Ohosumi, T., and Okukura, H. (1999). Analytical solutions of wave field in 3-dimensional Cartesian coordinate and their application to synthesis of seismic ground motions. *Journal of Structural Mechanics and Earthquake Engineering*, Japan Society of Civil Engineers, **612/I-46**, 99-108.

Harada, T. and Wang, H. (2005). Stiffness matrix based representation of wave motions in horizontally layered media, *ZISIN*. The Seismological Society of Japan, **57**, 387-392.

Heisey, J.S., Stokoe, II K.H., Hudoson, W.R., and Meyer, and A.H. (1982). Determination of in situ shear wave velocities from spectral analysis of surface waves. Research Report No. 256-2, *Center for Transportation Research*, The University of Texas.

Kausel, E. and Roesset, J.M. (1981). Stiffness matrices for layered soils. *Bull. of Seismological Soc. of America*, **71**, 1743-1761.

Marquardt, D.W. (1963). An algorithm for least squares estimation of nonlinear parameters, *Journal of Soc. Indust. Appl. Math.*, **11**, 431-441.

Nazarian, S., and Stokoe, II K.H. (1984). In situ shear wave velocities from spectral analysis of surface waves. *Proc. of the 8th Conference on Earthquake Engineering*, San Francisco, **3**, 38-45.